Optical Materials 84 (2018) 103–108

Contents lists available at ScienceDirect

Optical Materials

journal homepage: www.elsevier.com/locate/optmat

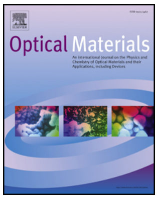

Origin of near-infrared luminescence in Bismuth-doped silica and germanosilicate glass fibers: Crystal field modeling

Oleksii V. Laguta[a,*], Igor M. Razdobreev[b]

[a] Institut für Physikalische Chemie, Universität Stuttgart, Pfaffenwardring 55, D-70569 Stuttgart, Germany
[b] Univ. Lille, CERLA, CNRS, UMR 8523 - PhLAM - Physique des Lasers, Atomes et Molecules, F59000, Lille, France

ARTICLE INFO

Keywords:
Bi^+ ion
Crystal field
Laser materials

ABSTRACT

Bismuth-doped silica-based glasses have already been proved to be promising materials for the fiber lasers and amplifiers operating in the near-infrared (NIR) spectral region. However, the development of such devices, which would have eligible efficiency, is impossible without a solid understanding of the NIR emitting center's nature. In the present work, based on the crystal field calculations we demonstrate that in silica and germanosilicate glasses this center is a univalent Bi ion affected by a rather strong local crystal field. According to our results, a transition from the first excited state to the ground state in Bi^+ causes the famous NIR photoluminescence. The relatively high degree of reduction of the spin-orbit coupling constant indicates, most probably, the formation of weak covalent bonding of Bi^+ with ions of the environment.

1. Introduction

Bismuth-doped silica glasses are very interesting optical materials due to their promising applications in advanced telecommunication systems [1], bioimaging [2], phosphors [3]. Based on such materials fiber lasers and amplifiers can potentially cover the inaccessible for rare-earth based devices spectral regions [4,5]. Nevertheless, despite the significant progress in the development of fiber devices based on Bi-doped glasses [4–7], there are several significant shortcomings. The lasing can be observed only at low levels of Bismuth doping, thus significantly long fibers are necessary to ensure the more or less efficient device operation. Also, the highest achieved efficiency is much lower comparing to the rare-earth analogues. Obviously, to explain these shortcomings the main unresolved problem, namely, the unknown nature of the near-infrared photoluminescence (PL) in Bi-doped silica glasses must be solved. Indeed, since its first observation [8,9], the list of hypotheses on the NIR PL origin became fairly long (Bismuth ions in various valence states, Bismuth dimers, point defects, etc.) [10–12]. It is important to note that with a high degree of reliability it was established that the optical centers in Bi-doped silica without other co-dopant and in germanosilicate glass are similar. In other words, the Bi-related optical centers in silica (BAC-Si) are the counterparts of that in GeO_2 glass network (BAC-Ge) [13]. At the same time, the optical centers in Bi-doped aluminosilicate (BAC-Al) and phosphosilicate (BAC-P) were recognized to have different properties.

Recently, the laser-induced bleaching and thermo-stimulated recovery of luminescent centers in bismuth-doped optical fibers were studied [14–16]. This very interesting phenomenon observed under excitation in the visible (530 or 407 nm) in germanosilicate fibers was explained as a result of a two-photon ionization process. The explanation is based on the assumption that the BAC-Si and BAC-Ge optical centers consist of a bismuth ion and one silica/germanium-related oxygen deficiency center (Si/Ge-ODC) [11]. The proposed model does not agree with the recent results of Romanov et al. [17] who studied the formation of the photoluminescent univalent bismuth silanolate by SiO_2 surface modification. This study clearly indicates that the resulting NIR PL is identical to that observed from BAC-Si in bulk Bi-doped silica. Moreover, it was shown later that the photo-bleaching effect can be observed in the BAC-Si under its resonant excitation in the NIR region. This finding implies that the active optical center does not necessarily consist of a bismuth ion and one Si/Ge-ODC, while the underlying mechanism of the photo-bleaching can be the loss of an excited electron due to the direct photo-ionization of Bi^{n+} ions [18]. The latter is in complete agreement with the results of Romanov et al. [17] and their assumption that Bi^+ ions are responsible for the NIR PL.

It should also be pointed out, that the assumption on the NIR PL optical centers consisting of Si/Ge-ODC (one or even two) and the Bi^{n+} ion was made [11,19] on the basis of a direct analogy with the works on atomic thallium centers in alkali halides [20] and lead centers in alkaline-earth fluorides [21,22]. First, it seems to us that such a direct analogy between ionic crystals and strongly covalent silica or germanosilicate glasses is somewhat controversial. On the other hand, it is not

---

[*] Corresponding author.
E-mail address: oleksii.laguta@ipc.uni-stuttgart.de (O.V. Laguta).

https://doi.org/10.1016/j.optmat.2018.06.047
Received 27 April 2018; Received in revised form 28 May 2018; Accepted 20 June 2018

clear why the simplest model of univalent bismuth is unsatisfactory for explaining the available experimental data.

In this paper, we perform a comparative analysis of the available experimental data and results of calculations in the framework of the simplest crystal field model for the Bi^+ ion. This study aims to show that not only the position of NIR absorption/excitation bands observed in experiment satisfactorily match the calculated ones but also their polarization properties inferred from magneto-optical experiments. We emphasize that in this paper only one center is considered, namely, responsible for the NIR lasing. Other centers, as the center responsible for the red PL [23], which can not be identified either as Bi^+ or as Bi^{2+} ions [24], or NIR centers in aluminosilicate and phosphosilicate glasses remain out of the scope of the present work.

2. Crystal field theory

The calculation of energy levels was performed in the frame of the crystal field theory of $p^{2,4}$ configuration developed by Davis et al. [25]. In this approach, the crystal field potential can be expanded in terms of the tensor operators $\mathbf{C}^{(k)}q$:

$$V = \sum_{i=1}^{2} \sum_{k} \sum_{q=-k}^{k} \mathbf{B}_q^k (\mathbf{C}_q^{(k)})_i, \tag{1}$$

where $i = 1,2$ is for two electrons of the Bi^+ ion [26]. Because we are dealing only with the p electrons ($k = 2$), five parameters $\mathbf{B}_q^2$ are present in the expansion (1). The component B_0^2 corresponds to the axial deformation of the crystal field, and it is non zero for any environment symmetry except for the cubic one. The components $B_{-2}^2 = B_{+2}^2$ are non vanishing only for six symmetry point groups (rhombic and monoclinic), namely, D_{2h}, C_{2h}, D_2, C_{2v}, C_2 and C_s [27]. These components, that will be addressed below as the "low symmetry" deformation, ensure complete removal of degeneracy for all excited states of Bi^+ ion. The remaining two components $B_{\pm 1}^2$ are non vanishing only for two lowest symmetry groups (triclinic), C_i and C_1, and they do not provide any new splitting. The last feature of the electronic configuration $p^{2,4}$ makes it possible to represent the crystal field potential in a simplified form, which ensures all possible splittings of all the states of Bi^+ ion:

$$V = \sum_{i=1}^{2} \{B_0^2 (C_0^{(2)})_i + B_2^2 [(C_2^{(2)})_i + (C_{-2}^{(2)})_i]\}. \tag{2}$$

It is well known that Bi^{n+} ions exhibit very strong spin-orbit coupling, which can be comparable to the crystal field interaction. For this reason, it is necessary to construct the full energy matrix using the complete basis set of all 15 free-ion Russell-Saunders states $|SLJM_J\rangle$, where S is the total spin, L is the total orbital angular momentum, J is the total angular momentum, and M_J is the projection of J on the z-axis. Following Davis et al. [25] we also neglect $B_{\pm 1}^2$ parameters in the crystal field potential decomposition and use the complete basis set of $|SLJM_J\rangle$ states. The resulting matrix (see Table S1 in Suppl. Mater.) has four adjustable parameters: the Slater electron-repulsion integral F_2, spin-orbit coupling constant λ and crystal field potential parameters B_0^2, B_2^2. The matrix can be easily diagonalized numerically for the given set of parameters. As a result, one obtains a set of eigenvalues (energy of levels) and eigenvectors (electronic states in the crystal field, see Table S2 in Suppl. Mater.). Obviously, these states are the linear combinations of atomic Russell-Saunders states $|SLJM_J\rangle$. It should be noted that the B_2^2 parameter usually gives a second order correction to the energy levels. It is responsible for the zero-field splitting (ZFS, here we mean *external magnetic* field) of doublets with $M_J \neq 0$. This splitting is not expected to be resolved by the conventional optical spectroscopy in the glass samples even at very low temperatures because of the strong inhomogeneous broadening. For this reason, at the first stage of our analysis only F_2, λ and B_0^2 parameters were varied to fit the calculated energy levels to the positions of experimentally measured absorption and excitation bands in optical spectroscopy. The variations of F_2 and λ were limited by ± 50% of their free-ion values, and B_0^2 was varied over the range of ± 20000 cm^{-1}. The parameter B_2^2 can be evaluated, for example, in the experiments on temperature and field dependences of magnetic circular polarization of luminescence (MCPL). The fitting procedure was realized with the Matlab simulated annealing function *"simulannealbnd"* in order to obtain the global minimum [28].

3. Bismuth-doped pure silica fiber without other co-dopant

In this Section we are interested in Bismuth-doped silica glass without other co-dopant. The first experimental investigation of photoluminescence in Bi-doped pure SiO_2 bulk glass was performed at low temperature [23], then soon after that, the photonic crystal fiber [29] and fibers fabricated by the powder-in-tube technique [30] were prepared and investigated at room temperature. Later the useful experimental data were reported in the subsequent works [7,31], in which the three-dimensional excitation-emission plots were constructed for different silica-based Bismuth-doped materials. Unfortunately, the latter experiments were performed only at room temperature and with the use of the low sensitivity equipment, so that some subtle features of the luminescence spectra were not detected. Finally, the magneto-optical experiments in this material were performed recently [24,32].

In this material, six absorption and excitation bands were reported previously [7,23,29,33]. Their energies positions (wavelengths) were collected in the first two columns of Table 1. We also added to this list the PL band at 843 nm, which is observed as a long wave shoulder in the PL spectrum recorded at low temperature under excitation at 375 or 415 nm as can be seen in Fig. 1 (see also Ref. 32). Note also, that the absorption and PL bands around 910 nm were also observed in fibers at ambient temperature (see, for example, Fig. 3 in Ref. [33]) and by Romanov et al. in univalent bismuth silanolate (see Figure S1 in Suppl. Mater.).

In Fig. 2 we show the energy level diagram of Bi^+ ion where the sub-state energies of three first excited states are shown as a function of the B_0^2 parameter. The axial crystal field splits the atomic states $^3P_1$, $^3P_2$ and $^1D_2$ into three singlet states, $1\Sigma^-$ ($^3P_1$, $M_J = 0$), $2\Sigma^+$ ($^3P_1$, $M_J = 0$), $3\Sigma^+$ ($^1D_2$, $M_J = 0$), and five doubly degenerate states, 1Π ($^3P_1$, $M_J = \pm 1$), 1Δ ($^3P_2$, $M_J = 2$), 2Π ($^3P_2$, $M_J = 1$), 2Δ ($^1D_2$, $M_J = 2$) and 3Π ($^1D_2$, $M_J = 1$). Hereinafter we use the $C_{\infty v}$ notation for the electronic states' designation. We recall that the additional splitting of levels with $M_J = \pm 1$ and $M_J = \pm 2$, when the parameter B_2^2 is taken into account, is imperceptible in the scale of the figure. At the same time, the MCPL experiments unequivocally revealed the multiplicity of excited electronic states related to 1420 and 810 nm bands [32]. As can be seen from Fig. 2, this imposes some restrictions on the possible values of the parameter B_0^2, which, as it turned out, must be positive, since only in this case the first excited state is degenerate. Thus, 810, 910 and 1420 nm absorption bands can be placed in correspondence with the doublets 2Π, 1Δ and 1Π, respectively. Varying the model parameters F_2,

Table 1

Measured and calculated energies of transitions in Bismuth-doped pure SiO_2. $F_2 = 994.9\ cm^{-1}$, $\lambda = 3760.8\ cm^{-1}$, $B_0^2 = 6976\ cm^{-1}$.

Measured (E_m)		Calculated (E_c)		$\frac{\lvert E_m - E_c \rvert}{E_m}$	Energy level
cm^{-1}	nm	cm^{-1}	nm		
41667	240	32882	304.1	2.1×10^{-1}	$4\Sigma^+$ ($^1S_0$)
26667	375	23273	429.7	1.3×10^{-1}	3Π ($^1D_2$, $M_J = \pm 1$)
24100	415	22592.2	442.6	6×10^{-2}	$3\Sigma^+$ ($^1D_2$, $M_J = 0$)
–	–	21810	458.5	–	2Δ ($^1D_2$, $M_J = \pm 2$)
12345	810	12350	809.7	4×10^{-5}	2Π ($^3P_2$, $M_J = \pm 1$)
11859[a]	843	11983	834.5	–	$2\Sigma^+$ ($^3P_2$, $M_J = 0$)
10990	910	10990.3	909.9	3×10^{-5}	1Δ ($^3P_2$, $M_J = \pm 2$)
–	–	9866.8	1013.5	–	$1\Sigma^-$ ($^3P_1$, $M_J = 0$)
7042	1420	7044	1419.6	3×10^{-4}	1Π ($^3P_1$, $M_J = \pm 1$)

[a] relaxed state observed in luminescence, see Fig. 1.